ISSN 0965-5441, Petroleum Chemistry, 2018, Vol. 58, No. 2, pp. 130–136. © Pleiades Publishing, Ltd., 2018.
Original Russian Text © E.Yu. Safronova, A.K. Osipov, A.B. Yaroslavtsev, 2018, published in Membrany i Membrannye Tekhnologii, 2018, Vol. 8, No. 1, pp. 34–41.

Short Side Chain Aquivion Perfluorinated Sulfonated Proton-Conductive Membranes: Transport and Mechanical Properties

E. Yu. Safronova[a, *], A. K. Osipov[a, b], and A. B. Yaroslavtsev[a, b, c]

[a] *Kurnakov Institute of General and Inorganic Chemistry, Russian Academy of Sciences, Moscow, 119991 Russia*
[b] *Department of Chemistry, Moscow State University, Moscow, 119991 Russia*
[c] *Institute of Problems of Chemical Physics, Russian Academy of Sciences, Chernogolovka, Moscow oblast, 142432 Russia*
**e-mail: safronova@igic.ras.ru*

Received September 6, 2017

Abstract—Data on the water uptake, proton conductivity, diffusion permeability, cation transport selectivity, and mechanical properties of short side chain Aquivion sulfonated perfluoropolymer membranes with an equivalent weight of 870 and 965 have been described. Properties of the membranes have been compared with those of a long side chain Nafion 212 membrane (equivalent weight of 1100). An increase in the equivalent weight leads to an increase in the sorption exchange capacity and water uptake of the membranes and a decrease in their proton conductivity. The conductivity of the Aquivion membrane with an equivalent weight of 870 is 1.4–1.5 times higher than that of the Nafion 212 membrane; it reaches 13.6 mS/cm in contact with water and 1.0 mS/cm at a relative humidity of 32% at 25°C. Diffusion permeability and cation transport selectivity exhibit a nonmonotonic dependence on the equivalent weight of the material. The lowest diffusion permeability, the highest Na^+ cation transport selectivity (99.5%), and the best mechanical properties have been found for the Aquivion membrane with an equivalent weight of 965, which is characterized by the highest degree of crystallinity.

Keywords: sulfonated perfluoropolymers, Aquivion, proton conductivity, selectivity, mechanical properties, Nafion
DOI: 10.1134/S0965544118020044

INTRODUCTION

Sulfonated perfluoropolymer membranes are of great interest to researchers owing to their fairly high transport properties, chemical and thermal stability and, as a consequence, a broad range of practical application. These membranes are used as a solid electrolyte in fuel cells and other devices for electrochemical current generation; in electrolytic cells, water treatment systems, and sensors; and in catalysis and gas separation processes [1–3]. The most commonly used and thoroughly studied materials of this type are Nafion membranes manufactured by DuPont (the United States) [4, 5]. They are based on polytetrafluoroethylene with relatively long side chains formed by ether and fluorocarbon groups end-capped with functional sulfo groups (Fig. 1a). Apparently, most of research papers and reviews addressing Nafion membranes in the last decades have been focused on their use in fuel cells [1, 2]. The requirements imposed on the electrolytes for fuel cells are as follows [6]:

—high proton conductivity, particularly at a low humidity and a high temperature;

—low permeability of fuel (hydrogen, methanol, oxygen);

—high chemical and thermal stability;

—low electronic conductivity; and

—desirably low cost.

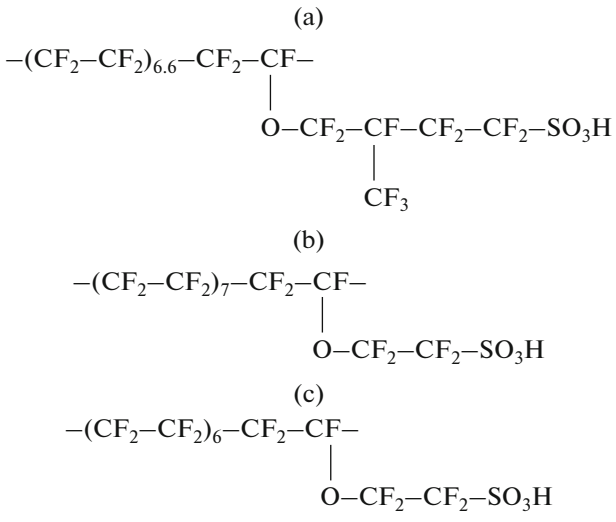

Fig. 1. Structure of (a) the Nafion membranes with an equivalent weight of 1100 and the Aquivion membranes with equivalent weights of (b) 965 and (c) 870.

Nafion membranes meet most of these requirements, except for the last-mentioned one; therefore, they are permanently attracting the close attention of researchers. For example, the proton conductivity of Nafion 212 membranes used in fuel cells is one of the highest proton conductivities exhibited by solid electrolytes [7]. Owing to the perfluorinated polymer chain, the heat resistance and chemical stability of these membranes are higher than the respective parameters of hydrocarbon and aromatic polymers [2, 8]. The gas permeability and electronic conductivity of these materials are relatively low. However, Nafion membranes have some disadvantages, which are being addressed through the efforts of a large number of research teams. One of the main disadvantages is a significant dependence of proton conductivity on the relative humidity of the environment; therefore, the material used in a fuel cell should be constantly moistened. Another important disadvantage is the limited operating temperature range. The glass transition temperature of the Nafion polymer is about 110°C [4]; in addition, high temperatures lead to the irreversible dehydration of the polymer and a deterioration of the properties of the material [9, 10]. To solve the problem of poisoning of a platinum catalyst in a fuel cell, which is caused by the irreversible sorption even of trace amounts of carbon monoxide present in the relatively cheap hydrogen produced by the reforming of hydrocarbons and alcohols, it is necessary to maintain the operating temperature of the system at a level not lower than 120°C. Another disadvantage of these membranes is their high cost. In this context, a wealth of attempts are being made to find materials that meet the requirements. In particular, Nafion membranes are modified with nanoparticles of various materials, such as hydrated oxides, inorganic acids and their acid salts, polyaniline, and carbon nanotubes [2, 11–18]. This approach has made it possible to synthesize materials whose properties are less dependent on humidity. Thus, the use of hybrid Nafion membranes containing hydrated silica nanoparticles provides an increase in the operating temperature of fuel cells to 130°C [19] and a decrease in the gas permeability and degradation rate of the material [20, 21].

Since the synthesis of hybrid materials makes the expensive electrolyte even more expensive, an approach aimed at the production of other polymers is being developed. An important direction is the design of materials that have a backbone similar to that of Nafion and a shorter side chain containing functional sulfo groups [22–24]. At present, these materials are also commercially available; they have different side chain lengths and equivalent weights (average polymer weight per functional group) and are produced under different names and trademarks (Dow, 3M, Aquivion, etc.). Figure 1 shows the structure of Aquivion membranes with an equivalent weight of 965 and 870. Advantages of these materials include a higher proton conductivity and a high ability to sorb water; these features, along with a higher degree of crystallinity and a higher glass transition temperature, open up prospects for using these materials in fuel cells at higher temperatures [24]. However, the number of reports on the study of the properties of short side chain perfluorinated sulfonated polymers is incomparably smaller than the number of reports on Nafion; in addition, the data commonly concern only the water uptake, conductivity, and characteristics of fuel cells. Published data on diffusion permeability, selectivity, and mechanical properties are quite scarce. Since the properties of perfluorinated sulfonated polymers significantly depend on their preparation technique and history [25–27], it is reasonable to conduct an integrated study of their properties.

The aim of this study was to investigate the water uptake and transport (proton conductivity, diffusion permeability, selectivity) and mechanical properties of short side chain Aquivion perfluorinated sulfonated membranes with different equivalent weights and compare these materials with the Nafion 212 membrane.

EXPERIMENTAL

Materials

Aquivion E87-05S membranes (Solway, equivalent weight of 879), Aquivion E98-05S (Solway, equivalent weight of 965), and Nafion 212 membranes (DuPont, equivalent weight of 1100) were used. All the materials in a dry state have the same thickness (about 55 ± 3 μm). The following reagents were used for membrane conditioning and experiments: hydrogen peroxide (reagent grade, Khimmed); nitric acid (reagent grade, Khimmed); sulfuric acid (reagent grade, Khimmed); sodium chloride (special purity grade, Khimmed); and deionized water (resistance of 18.2 MΩ).

Membrane Conditioning

Prior to experiments, the membranes were subjected to conditioning as described in [28]. The films were boiled in a 3% hydrogen peroxide solution for 1 h and then successively held in a 7 M nitric acid solution at room temperature for 30 min, in a 1 M hydrochloric acid solution at 80°C for 1 h, and in water at 90°C for 1 h. To convert the membranes to the sodium form, they were held in a 2 M NaCl solution for 72 h.

Investigation Procedures

The thermal analysis of the samples was conducted using a Netzsch-TG 209 F1 thermobalance. The experiment was conducted in platinum crucibles in an argon atmosphere in the temperature range of 25–200°C. The heating rate was 10 K/min. The water uptake of the membranes was determined from the difference in weight before the heat treatment and

after holding at 200°C. The water uptake of the samples was studied both immediately after their long-term contact with water (excess water was removed from the surface with filter paper before the experiment) and after pre-equilibration at a low relative humidity of RH = 32%. To this end, the membranes were held in a desiccator at a relative humidity provided by a saturated $CaCl_2$ solution.

To determine the ion exchange capacity (IEC, meq/g), a weighed portion (~0.3 g) of the membrane in the dry state was held in 50 mL of a 0.1 M NaCl solution (V_{NaCl}, L) under constant stirring for 12 h. After that, the salt solution and the membrane were titrated with a 0.01 M NaOH solution. The ion exchange capacity (meq/g) was calculated on a dry resin basis [29].

The ionic conductivity of the membranes in the H^+ form was determined at varying temperature in a range of 20–99°C at RH = 100% in contact with deionized water and in a temperature range of 25–45°C at RH = 95 and 32% in the air. Required humidity and temperature were provided by using a Binder MKF115 constant climate chamber (humidity control accuracy of ±2.5%). Measurements were conducted using an Elins E-1500 AC bridge (frequency range of 10 Hz to 2 MHz) on symmetrical carbon/membrane/carbon cells with an active surface area of 1 cm^2. Conductivity value (Cm/cm) was calculated from the resistance found via extrapolating the impedance hodographs to the axis of active resistances. The error in the determination of the conductivity value was less than 10%.

To determine diffusion permeability, the sample was placed between two compartments; each of the compartments had a volume of 32 cm^3. One of the compartments was filled with a 0.1 M HCl solution; the other, with deionized water; the liquids were constantly stirred using magnetic stirrers. In the experiment, the change in the pH value in the compartment initially containing deionized water was measured using an Expert-001 pH meter (Econix-Expert). The pH meter was calibrated using standard buffer solutions. The experiment was conducted at room temperature (about 25°C). The diffusion permeability of the membranes was calculated by the formula

$$P = \frac{dc}{dt}\frac{Vl}{S\Delta c}, \quad (1)$$

where V is the solution volume, cm^3; l is the membrane thickness, cm; Δc is the concentration gradient, mol/cm^3; and t is the time, s (error in the determination of the P value is less than 1%).

The membrane potential of the studied materials was determined at a temperature of 25°C. The samples in the sodium form were preliminary held in a 0.5 M NaCl solution for 12 h; after that, they were placed in a cell similar to that used to determine the diffusion permeability. The NaCl solution concentration was 0.1 M in one compartment and 0.5 M in the other. An Ag–AgCl electrode (Mettler-Toledo InLab Reference Pro) was placed in each of the compartments. The membrane potential between the electrodes was measured as a function of time using an Elins P30J potentiostat/galvanostat. Cation transport numbers (t_+) were determined as described in [30] and calculated by the formula

$$t^+ = \frac{\left[E_m \Big/ \left(\frac{RT}{F}\ln\frac{a_1}{a_2}\right)\right] + 1}{2}, \quad (2)$$

where E_m is the membrane potential, mV; R is the universal gas constant; T is the absolute temperature, K; F is the Faraday constant; and a_1 and a_2 are the electrolyte activity (found by extrapolation with a continuous function of tabulated values; $a_1 > a_2$; a_1 (0.5 M NaCl) = 0.338 and a_2 (0.1 M NaCl) = 0.0778). The accuracy of determination of t^+ was ±0.2%.

The mechanical properties of the membranes were studied using a Tinius Olsen H5KT tensile testing machine with a 100-N force sensor at a temperature of $T = 27 \pm 2$°C and RH = 20 ± 2%. The films were previously held at RH = 95%. Rectangular samples with a length of 80 mm (gage length of 60 mm) and a width of 10 mm were used. Ten experiments were conducted for each of the membranes. Thickness and width were determined immediately before the experiment as an average value at five points along the entire length (using a Mitutoyo micrometer; accuracy of determination of 0.001 mm). Young's modulus was determined from the slope of the stress–strain curve in the elastic strain region. Ultimate forced elasticity was determined as the point of intersection of the tangents to the portions corresponding to the elastic and plastic strains. Average values for each set of samples were calculated; measurement error was estimated according to Student's distribution.

RESULTS AND DISCUSSION

IEC and Water Uptake

The IEC and water uptake of the studied materials are listed in Table 1. IEC decreases with an increase in the equivalent weight from 1.08 mg-equiv/g for Aquivion 87 to 0.87 mg-equiv/g for Nafion 212. With an increase in the equivalent weight of the membranes, their water uptake decreases both in contact with water and at a low humidity; this finding is attributed to a decrease in the number of functional groups that contribute to the sorption of water molecules. In this case, the number of water molecules per sulfo group also decreases with increasing equivalent weight. This feature is associated with an increase in the fraction of polymer chains that limit the deformability of the membrane matrix during swelling.

Table 1. Equivalent weight, ion exchange capacity, and water uptake of the studied membranes

Sample	Equivalent weight, arb. units	IEC, meq/g	$W(H_2O)$ in contact with water, %	$n(H_2O/-SO_3H)$ in contact with water	$W(H_2O)$ at RH = 32%, %	$n(H_2O/-SO_3H)$ at RH = 32%
Aquivion 87	879	1.08	28.0	14.4	5.6	3.0
Aquivion 98	965	0.96	24.2	14.0	4.1	2.5
Nafion 212	1100	0.87	21.6	13.8	3.3	2.2

Proton Conductivity

The temperature dependences of the proton conductivity of the membranes measured at varying humidity are shown in Fig. 2. With an increase in the equivalent weight of the polymer, the conductivity decreases in the order: Aquivion 87 > Aquivion 98 > Nafion 212. The conductivity of the Nafion 212 membrane at 25°C is 1.4–1.5 times lower than that of Aquivion 87. The activation energy of conductivity slightly increases in the same order; for example, in contact with water, it increases from 6.7 ± 0.2 kJ/mol for Aquivion 87 to 7.7 ± 0.3 kJ/mol for Nafion 212. A decrease in conductivity and an increase in the activation energy of conductivity with an increase in the equivalent weight of the polymer are attributed to a decrease in the density of functional groups and in the water uptake of the materials.

With a decrease in relative humidity, the conductivity of the samples significantly decreases owing to membrane dehydration (Fig. 2). Thus, at room temperature, the conductivity values measured in contact with water and at RH = 95% differ by 1.7–2.1 times; in contact with water and at RH = 32%, they differ by 13–14 times. The conductivity decreases owing to the dehydration of the samples and a change in the proton transport mechanism. Thus, at the high humidity, the number of water molecules per functional sulfo group is 13–14 (Table 1) and the proton transport obeys the Grotthuss mechanism, whereas at RH = 32%, the proton transport occurs by hopping from one $H(H_2O)_n^+$ group to another [31]. At the same time, a considerable change in the water uptake and conductivity of the samples in contact with water and at RH = 95% is determined by the Schroeder paradox [32] associated with the exit of a portion of the protons from the membrane and the expansion of the pores due to electrostatic repulsion.

Table 2. Diffusion permeability of 0.1 M HCl across the membranes into water

Sample	$P \times 10^8$ (0.1 HCl) cm^2/s
Aquivion 87	15.6
Aquivion 98	5.6
Nafion 212	10.1

At RH = 95%, the dependence of the logarithm of conductivity on the $1000/T$ is not linear (Fig. 2b). Deviation from a linear dependence occurs owing to the degradation of the material; it is associated with the dehydration of the samples at high temperatures. Similar effects were observed in [10, 26]. This effect is most pronounced for the Aquivion 87 membrane, which has the lowest equivalent weight.

Diffusion Permeability and Cation Transport Selectivity

Table 2 shows the diffusion permeability of a 0.1 M HCl solution. The diffusion permeability of the membranes nonmonotonically depends on the equivalent weight of the polymer and increases almost threefold in the order: Aquivion 98 < Nafion 212 < Aquivion 87. Since the samples are cation-exchange membranes, the process rate is limited by the permeability of Cl^- anions and comparison of the diffusion permeability with the conductivity represents the cation transport selectivity. The highest selectivity—t_+ (Na^+) ≈ 99.5%—is observed for the Aquivion 98 membrane, which exhibits the lowest HCl solution permeability; the lowest selectivity is found for the Aquivion 87 membrane (Table 3).

Cation transport mostly occurs within the thin Debye layer localized near the pore walls, whereas the anions, conversely, are displaced from this region owing to repulsion from the similarly charged pore walls and can move only in the middle of the pores containing an electrically neutral solution [33]. An increase in the equivalent weight of the polymer upon switching from Aquivion 87 to Aquivion 98 leads to a decrease in the water uptake (Table 1) and, therefore, in the pore size [34]. As a consequence, the largest volume of the electrically neutral solution, the highest anion transport, and the best diffusion permeability are exhibited by the Aquivion 87 membrane, which has the lowest equivalent weight.

However, according to small-angle X-ray scattering data, the microstructure of the Aquivion membranes somewhat differs from that of Nafion; differences are observed both in the degree of crystallinity and the number of ion-exchange groups and in the side chain mobility. According to [35, 36], short chains restrict the segmental mobility of sulfo groups; therefore, smaller pores are formed in the Aquivion 98

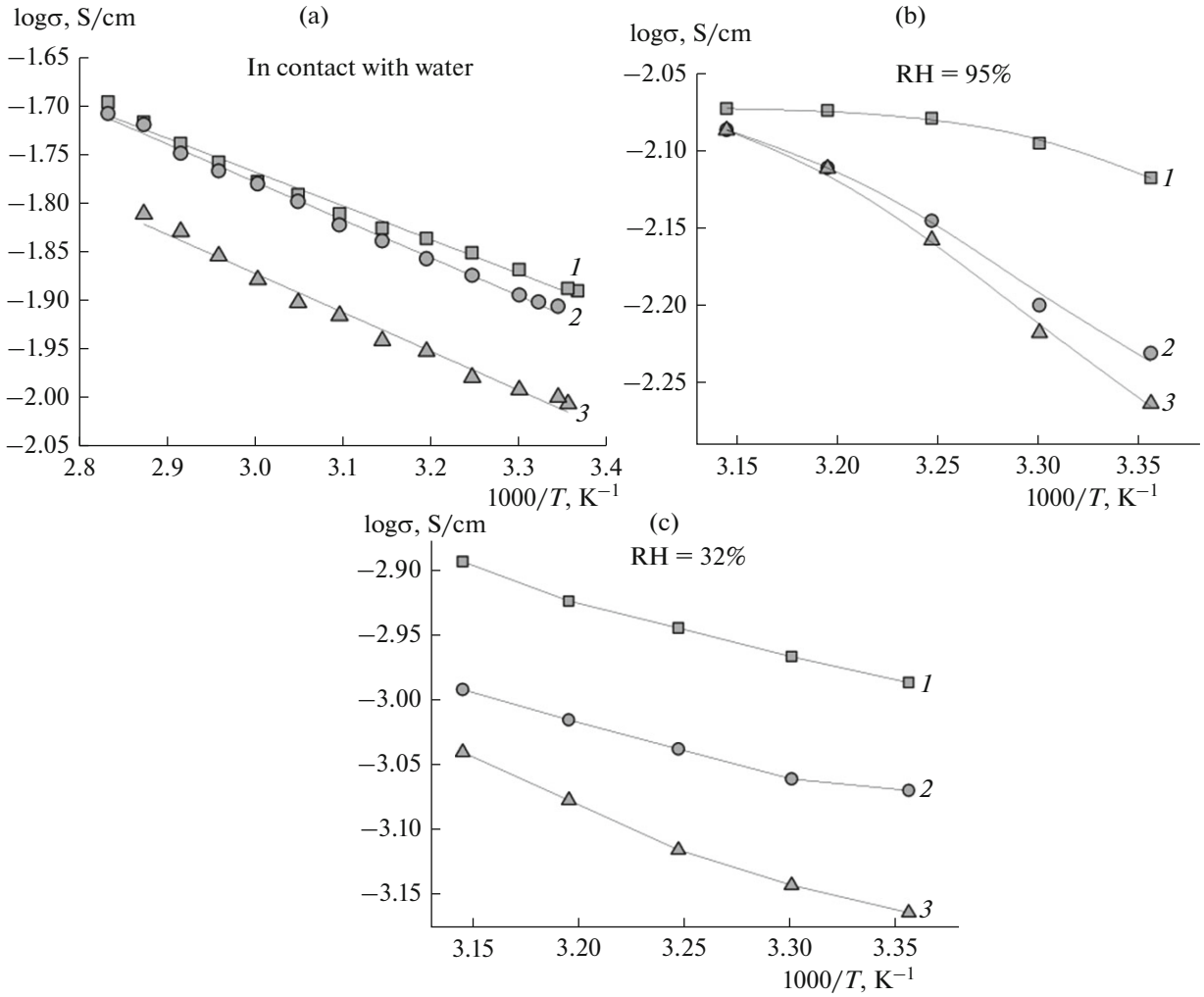

Fig. 2. Temperature dependences of proton conductivity measured (a) in contact with water and at RH = (b) 95 and (c) 32% for (*1*) the Aquivion 87, (*2*) Aquivion 98, and (*3*) Nafion 212 membranes.

membranes; accordingly, the volume of the electrically neutral solution in them decreases. Apparently, it is this feature that is responsible for the more hindered anion transport in the Aquivion 98 membranes despite the fact that their water uptake is higher. This feature leads to the highest selectivity for transport processes in these membranes.

The transport of small nonpolar molecules (hydrogen, oxygen) or molecules with a lower polarity than that of water (methanol), which are used in electrochemical processes in fuel cells, occurs through the electrically neutral solution, similar to anion transport [36]. Therefore, it is reasonable to expect that the permeability of these molecules across the Aquivion 98 membranes will be less than the permeability across Nafion 212.

Mechanical Properties

Typical stress–strain plots for the studied membranes are shown in Fig. 3. At low strains (up to 10%), a linear dependence on the stress is observed; it corresponds to the elastic region and reversible deformations. After achieving the ultimate forced elasticity, a change in the slope is observed; further stretching leads to irreversible deformations of the samples. The formation and propagation of microcracks lead to the degradation of the material.

The breaking stress and breaking strain values significantly differ from experiment to experiment, while other parameters and the behavior of the curves are nearly same. This finding is attributed to the heteroge-

Table 3. Transport numbers (%) of Na^+ ions across the membranes

Sample	t^+ (Na^+), %
Aquivion 87	95.9
Aquivion 98	99.5
Nafion 212	97.3

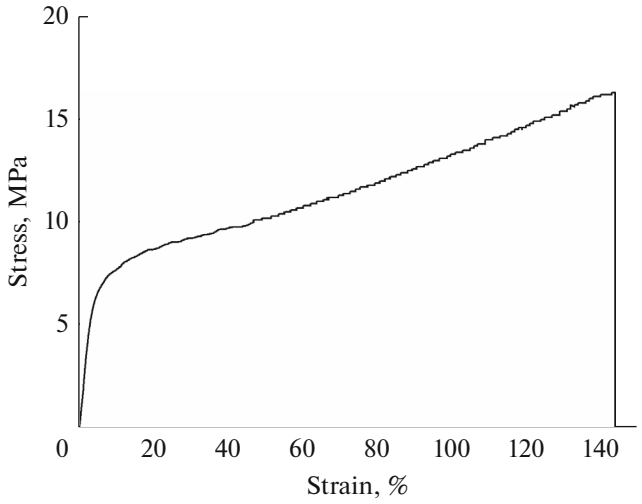

Fig. 3. Typical stress–strain curve for the Aquivion 87 membrane.

neous structure of the membranes. The system of hydrophilic pores and channels in them can be regarded as an analog of microcracks, which are known to substantially decrease the strength of solids. Since the arrangement of the pores and their junction geometry are determined by statistical regularities, some samples are destroyed even at relatively low loads, while other samples are significantly stronger. The break stress values for the studied membranes differ within the limits of error. However, it should be noted that the Aquivion 98 membranes, which have the highest degree of crystallinity [24], are the most durable of all the studied membranes. A decrease in the number of ion-exchange groups (increase in the equivalent weight) leads to the weakening of the interaction between them and an increase in the relative crystallinity of the materials. The degree of crystallinity of short side chain materials is higher than that of long side chain materials because, during crystallization, the side chain packing in the backbone for the former is significantly simpler than that for the latter [24].

The Young's modulus and proportional limit stress values for the studied membranes also differ only slightly from one another (Table 4). However, the Aquivion 98 membrane exhibits somewhat higher Young's modulus and proportional limit stress values owing to the higher degree of crystallinity of the material.

Table 4. Young's modulus and proportional limit stress of the membranes

Sample	Young's modulus, MPa	Proportional limit stress, MPa
Aquivion 87	134 ± 22	6.4 ± 0.6
Aquivion 98	156 ± 16	6.7 ± 0.3
Nafion 212	139 ± 10	6.0 ± 0.3

CONCLUSIONS

The water uptake and transport and mechanical properties of short side chain Aquivion perfluorosulfonic membranes with an equivalent weight of 879 and 965 and long side chain Nafion 212 membranes (equivalent weight of 1100) have been studied. The ion exchange capacity, water uptake, and proton conductivity monotonically decrease with increasing equivalent weight both at high and low relative humidity. At RH = 32%, the conductivity is 13 to 14 times lower than in the case of contact with water. The lowest diffusion permeability and the highest cation transport selectivity are observed for the Aquivion membrane with an equivalent weight of 965; this finding is attributed to the fact that the system of pores and channels in this material is less branched than that of the other membranes. This feature, along with fairly high mechanical properties, makes this material the most promising for use in electrochemical devices, in particular, as an electrolyte in fuel cells.

ACKNOWLEDGMENTS

This work was supported by the Russian Science Foundation, project no. 17-79-30054.

REFERENCES

1. S. J. Peighambardoust, S. Rowshanzamir, and M. Amjadi, Int. J. Hydrogen Energy **35**, 9349 (2010).
2. S. Bose, T. Kuila, T. X. Hien Nguyen, et al., Prog. Polym. Sci. **36**, 813 (2011).
3. E. Yu. Safronova and A. B. Yaroslavtsev, Pet. Chem. **56**, 281 (2016).
4. K. A. Mauritz and R. B. Moore, Chem. Rev. **104**, 4535 (2004).
5. Deuk Ju Kim, Min Jae Jo, and Sang Yong Nam, J. Ind. Eng. Chem. **21**, 36 (2015).
6. C. M. Branco, A. El-kharouf, and S. Du, in *Reference Module in Materials Science and Materials Engineering.*, Ed. by S. Hashmi (Elsevier, 2017). doi 10.1016/b978-0-12-803581-8.09261-4
7. A. B. Yaroslavtsev, Russ. Chem. Rev. **78** (11), 1013 (2009).
8. G. Pourcelly, Pet. Chem. **51**, 480 (2011).
9. G. Alberti, R. Narducci, and M. Sganappa, J. Power Sources **178**, 575 (2008).
10. E. Safronova, D. Safronov, A. Lysova, et al., Sens. Actuators B **240**, 1016 (2017).
11. B. P. Tripathi and V. K. Shahi, Prog. Polym. Sci. **36**, 945 (2011).
12. E. Yu. Safronova and A. B. Yaroslavtsev, Solid State Ionics **221**, 6 (2012).

13. V. D. Noto, N. Boaretto, E. Negro, et al., Int. J. Hydrogen Energy **37**, 6215 (2012).
14. H. Strathmann, A. Grabowski, and G. Eigenberger, J. Ind. Eng. Chem. Res. **52**, 10364 (2013).
15. B. R. Matos, R. A. Isidoro, E. I. Santiago, et al., Int. J. Hydrogen Energy **40**, 1859 (2015).
16. E. Gerasimova, E. Safronova, A. Ukshe, et al., Chem. Eng. J. **305**, 121 (2016).
17. I. A. Prikhno, E. Yu. Safronova, and A. B. Yaroslavtsev, Int. J. Hydrogen Energy **41**, 15585 (2016).
18. E. Yu. Safronova, I. A. Stenina, and A. B. Yaroslavtsev, Pet. Chem. **57**, 299 (2017).
19. C. C. Ke, X. J. Li, S. G. Qu, et al., Polym. Adv. Technol. **23**, 92 (2012).
20. H. Tang, Z. Wan, M. Pan, and S. P. Jiang, Electrochem. Commun. **9**, 2003 (2007).
21. A. D'Epifanio, B. Mecher, E. Fabbri, et al., J. Electrochem. Soc. **154**, B1148 (2007).
22. K. D. Kreuer, M. Schuster, B. Obliers, et al., J. Power Sources **178**, 499 (2008).
23. P. Xiao, J. Li, H. Tang, et al., J. Membr. Sci. **442**, 65 (2013).
24. J. Li, M. Pan, and H. Tang, RSC Adv. **4**, 3944 (2014).
25. N. Berezina, S. Timofeev, and N. Kononenko, J. Membr. Sci. **209**, 509 (2002).
26. G. Alberti, R. Narducci, and M. Sganappa, J. Power Sources **178**, 575 (2008).
27. R. Kuwertz, C. Kirstein, T. Turek, and U. Kunz, J. Membr. Sci. **500**, 225 (2016).
28. A. Skulimowska, M. Dupont, M. Zaton, et al., Int. J. Hydrogen Energy **39**, 6307 (2014).
29. M. Amirinejad, S. S. Madaeni, M. A. Navarra, et al., J. Power Sources **196**, 988 (2011).
30. M. Geise, H. J. Cassady, D. R. Paul, et al., Phys. Chem. Chem. Phys. **16**, 21673 (2014).
31. V. I. Volkov, E. V. Volkov, S. V. Timofeev, et al., Russ. J. Inorg. Chem. **55**, 315 (2010).
32. V. I. Roldugin and L. V. Karpenko-Jereb, Colloid J. **78**, 795 (2016).
33. A. B. Yaroslavtsev and V. V. Nikonenko, Nanotechnol. Russ. **4**, 137 (2009).
34. G. Gebel and R. B. Moore, Macromolecules **33**, 4850 (2000).
35. K. D. Kreuer, M. Schuster, B. Obliers, et al., J. Power Sources **178**, 499 (2008).
36. M. K. Mistry, N. R. Choudhury, N. K. Dutta, and R. Knott, Langmuir **26**, 19073 (2010).

Translated by M. Timoshinina